# Atmospheric Propagation of Two $CO_2$ Laser Pulses

M. Autric,* J-P. Caressa,† D. Dufresne,‡ and Ph. Bournot§
*Institute of Fluid Mechanics, Marseille, France*

**An experimental investigation has been conducted to study the propagation of a high-energy laser beam ($\bar{\phi}_B \geq 10^8$ W/cm$^2$; $\bar{F}_B \geq 10$ J/cm$^2$) in the atmosphere. At these intensities and fluence levels air breakdown can occur because of the interaction of the intense radiation with the aerosol particles naturally suspended in the path of the beam. An air plasma is created, which expands rapidly and consequently can have a detrimental effect on the energy propagation. This paper reports, first, the energy transmitted through the breakdown plasma as a function of the incident average energy density ($E_T/E_I < 15\%$ for $\bar{F}_I > 300$ J/cm$^2$) and second, the possibility of increasing the transmission of the incident energy by the application of a precursor pulse as a function of the double-pulse separation time (controllable from a few microseconds to 1/10 s). In our particular experiment, the maximum increase (by a factor of three) is observed for $\Delta t = 100$-$200$ $\mu$s, an effect due to the cleaning effect of the first pulse by vaporizing aqueous aerosol particles.**

## Nomenclature

| | |
|---|---|
| $E_I, E_T$ | = incident, transmitted energy, J |
| $E_I^*$ | = 80% of the total incident energy |
| $E_T^\ddagger$ | = transmitted laser energy with precursor pulse |
| $\bar{F}_B$ | = average breakdown threshold (fluence) |
| $F_I, F_T$ | = incident, transmitted energy density, J/cm$^2$ |
| $\bar{F}_I, \bar{F}_T$ | = average incident and transmitted energy density values on the focal spot |
| $\overline{F_T^\ddagger}$ | = average transmitted energy density with precursor pulse |
| FWHM | = full width at half maximum |
| $f$ | = focal length in meter |
| $f/D$ | = f-number of the optical system |
| RH | = relative humidity of air |
| $S^*$ | = focal spot area that includes approximately 80% of the total incident energy |
| $\Delta t$ | = double-pulse separation time |
| $W_I(t), W_T(t)$ | = incident, transmitted laser powers, W/cm$^2$ |
| $\tau_P$ | = pulse length |
| $\bar{\phi}_B$ | = average breakdown threshold (intensity) |
| $\phi_T^\ddagger$ | = maximum transmitted intensity with precursor pulse |
| $\bar{\phi}_{\text{peak}}$ | = maximum intenstiy (top of the spike of the pulse) |
| $\bar{\phi}_{\text{tail}}$ | = average intensity during the tail of the laser pulse. |

## Introduction

PULSED high-power $CO_2$ laser beams propagating through the Earth's atmosphere can be affected by different linear or nonlinear phenomena such as aerosol and molecular absorption, scattering, turbulence, or thermal blooming. The attenuation by the only significant molecular absorbers present in the atmosphere ($H_2O$, $CO_2$, and $N_2$) is relatively low.

At very high fluxes ($10^7$-$10^8$ W/cm$^2$) laser-induced breakdown can occur because of the interaction of the intense radiation with the aerosol particles naturally suspended in the path of the beam.[1-4] The study of this phenomenon and of its importance is the purpose of our work. Numerous published studies have shown that the presence of these microscopic particles substantially reduces the breakdown threshold.[5-8]

Previously, we have determined in a realistic atmosphere outside the laboratory the threshold values necessary for the air breakdown (intensity $1\text{-}2 \times 10^8$ W/cm$^2$, fluence 3-5 J/cm$^2$, and $\tau_p = 50$ ns).[9] The experimental results have taken into account the diffraction of the annular apertured beam, spherical aberration phenomena induced by the focusing optical system, spatial and temporal energy density distributions in the focal spot, size of the focal volume, size and distribution of the atmospheric aerosol particles suspended in the breakdown volume.

When the intensity and fluence levels are high enough to cause the breakdown initiated by the aerosol particles, a high-pressure, high-density air plasma is created. This plasma absorbs the incident energy according to the inverse bremsstrahlung absorption process and subsequently develops axially and radially.[6,10-13] The development of the plasma during the first part of the interaction (supported regime $t < \tau_p$) has been numerically studied considering three well-known hydrodynamical models (one-dimensional laser-supported detonation wave,[14] two-dimensional laser-supported absorption wave,[15] and unsteady laser-supported wave with spherical symmetry[16]) and compared with experiments (time-integrated, streak, and schlieren photographs recording the plasma luminosity and shock wave) to evaluate the accuracy of these models.[17] Air plasma propagating from the initiation sites grows to the point where it almost completely blocks the incident energy.

In the present paper we report experimental results concerning, first, the energy transmitted through the breakdown plasma as a function of the incident average energy density in the focal spot and, second, the possibility of increasing the transmission of the incident energy by the application of a precursor pulse.

## Experimental Setup

The following experiments have been performed with two TEA $CO_2$ lasers, the first of which is capable of producing up to 200 J with a pulse duration of 2.5 $\mu$s (laser COCA) and the second up to 2 KJ in 10 $\mu$s (laser TEKILA). Both pulses

Presented as Paper 82-0896 at the AIAA/ASME Third Joint Thermophysics, Fluids, Plasma and Heat Transfer Conference, St. Louis, Mo., June 7-11, 1982; submitted June 17, 1982; revision received Feb. 10, 1983. 

*Research Scientist, Centre National de La Recherche Scientifique. Member AIAA.

†Research Scientist, Centre National de La Recherche Scientifique.

‡Maître-Assistant, Université Aix-Marseille II. Member AIAA.

§Maître-Assistant, Université Aix-Marseille II (presently at the Faculté des Sciences et Techniques Monastir, Tunisia).

consist of an initial high-power gain-switched spike followed by a high-energy tail. The annular-shaped beams are near diffraction limited. (External diameter $D_{COCA} = 100$ mm, $D_{TEKILA} = 150$ mm.) Each laser beam has its own diagnostic system including a calorimeter for energy control (shot-to-shot energy variation is better than 10%) and a photon-drag detector for power control (the temporal shape of the output pulse is very reproducible). Oscillograms of typical laser pulse time history are shown in Fig. 1.

In order to focus the laser beam at various distances inside and outside the laboratory, two types of optical systems have been used: 1) spherical concave mirrors of focal lengths 5, 10, and 13 m; 2) optical systems with a "Cassegrain" configuration, the focal length of which is controlled by varying the intermirror distance. These systems are composed by an on-axis parabolic mirror $f/1.5$ ($\Phi = 0.65$ m, $f = 1$ m) coupled with an hyperbolic convex mirror. Experiments have been conducted at distances up to 214 m for the laser COCA resulting in an f-number of the system up to 428 (beam diameter on the pupil of the $5\times$ telescope $= 0.5$ m), and up to 62 m for the laser TEKILA resulting in a f-number of 103 (beam diameter on the pupil of the $4\times$ telescope, $D = 0.60$ m). The experimental setup is schematically represented in Fig. 2.

## Experimental Results

Measurements of laser energy transmitted through the breakdown plasma have been made by using two independent methods:

1) Direct measurement of the incident and transmitted energy by means of calorimeters

$$E_T/E_I = \bar{F}_T/\bar{F}_I$$

where $\bar{F}_I$ (J/cm$^2$) $= E_I^*/S^*$. $E_I^* = 80\%\ E_{I\text{total}}$ and $S^*$ is focal spot area that includes approximately 80% of the total incident energy.

2) Measurement of the temporal variation of the incident and the transmitted power by means of photon-drag detectors on which the pulse is refocused after attenuation. The energy balance can be evaluated by successive temporal integration of the photon-drag recordings

$$\frac{E_T(t)}{E_I(t)} = \int_0^{\tau_P} W_T(t)\,dt \Big/ \int_0^{\tau_P} W_I(t)\,dt$$

For both types of measurements, the laser pulse transmitted through the breakdown plasma is focused onto the photon-drag detector or the calorimeter by means of a 18 cm diam 1 m focal length mirror (M9 in Fig. 2 and M6 in Fig. 8) (the diameter of the laser spot at surface of this collecting mirror is maintained to about 6 cm). We have previously verified that the scattering of the radiation out of the field of the focusing mirror is negligible. Burn patterns produced on the thermosensitive surface of photographic paper and detailed measurements of the transmitted laser light both in space and in time have shown clear evidence that unabsorbed laser energy arrives in the central region of the beam cross section after passing through the formed plasma balls. The aspects of beam trapping and significant energy absorption have been demonstrated.[18] Measurements of the transmitted energy have been carried out as a function of the incident average fluence $\bar{F}_I$. In order to vary fluence values in the focal volume, it is necessary to control either the total energy of the pulse (laser COCA 0-200 J, laser TEKILA 0-2 kJ) by inserting terphane attenuators or the focal spot area [proporational to $(f/D)^2$] by varying the f-number of the optical system.

Figure 3 shows the experimental data obtained with COCA laser pulses ($0 < E_I < 200$ J, $0.11 < S^* < 2.2$ cm$^2$) inside the laboratory [$f = 5$ m ($f/D = 50$)], $f = 10$ m ($f/D = 100$) with normal laboratory conditions (20° C air temperature, 40% relative humidity); and outside the laboratory [$f = 55$ m

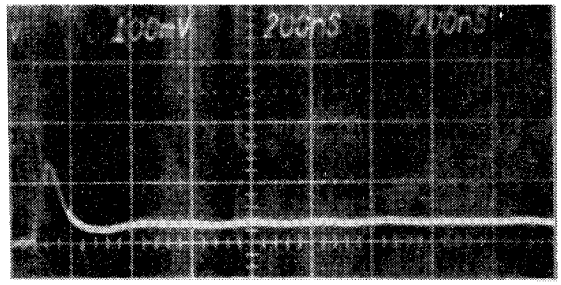

a) 200 ns/division.

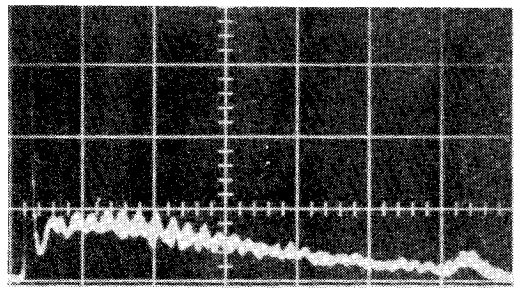

b) 1 μs/division.

**Fig. 1 Incident $CO_2$ laser pulse shape. For laser TEKILA, $E_I = 1150$ J; $\tau_p = 6$ μs; spike rise time in the ramping portion ≃ 80 ns, 80 ns, FWHM; peak power ≃ $10^9$ W; ratio of peak power to tail power ≃ 4; ratio of spike energy to total energy ≃ 0.1. For Laser COCA, $E_I = 160$ J; $\tau_p = 2.5$ μs spike rise time in ramping portion 50 ns; FWHM ≃ 50 ns; peak power $0.5\times10^9$ W; ratio of peak power to tail power ≃ 5; ratio of spike energy to total energy ≃ 0.2.**

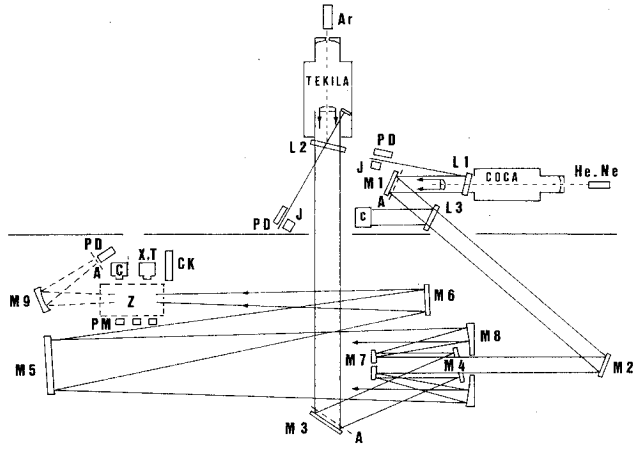


**Fig. 2 Experimental setup. Key: A-attenuators; L1, L2, L3-NaCl windows; PD-photon-drag detector; c, J-calorimeters; PM-photomultipliers; C, X, t-cameras; CK-particles optical counter; M1 to M6-plane mirrors; M7-hyperbolic convex mirror; M8-parabolic concave mirror; M9-spherical concave mirror; Ar, He-Ne-laser probe; Z-interaction zone. The same experimental arrangement is used for both lasers (except that the power of the telescope is altered by changing the hyperbolic mirror M7).**

($f/D = 135$)], $f = 110$ m ($f/D = 270$) with atmospheric conditions of approximately 10°C air temperature and 80% relative humidity. For these conditions, air breakdown was initiated by the spike (50 ns FWHM) early in the pulse for average intensity and fluence values of $1\text{-}2\times10^8$ W/cm$^2$ and 3-5 J/cm$^2$, respectively.[9] The results show that the transmission decreases rapidly as soon as breakdown occurs.

In the same way, Fig. 4 shows the experimental data obtained with the TEKILA pulse ($0 < E_I < 2$ kJ, $S^* = 0.24$ and 2 cm$^2$) inside the laboratory [$f = 13$ m ($f/D = 87$)] with standard conditions (20°C, 40% RH) and outside the laboratory [$f = 62$ m ($f/D = 103$)] with atmospheric conditions of approximately 10°C, 65% RH. We note that the ratio of transmitted energy

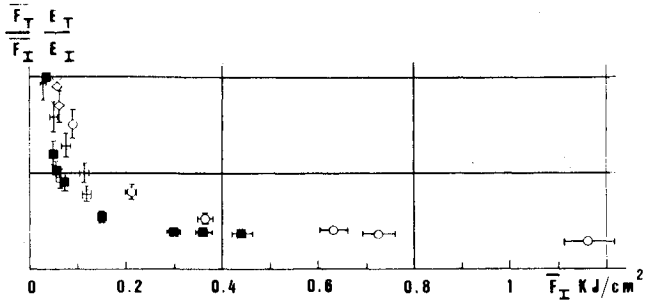


Fig. 3 Ratio of transmitted energy to incident energy as a function of incident fluence. Experimental conditions: $0<E_I<200$ J; ○ $f=5$ m, $S^*=0.11$ cm²; ■ $f=10$ m, $S^*=0.40$ cm²; ⊞ $+f$: 55 m, $S^*=1$ cm²; ◇ $f=110$ m, $S^*=2.2$ cm². The error bars show the estimated uncertainty of the energy measurements (10%) and the focal spot size (10%).

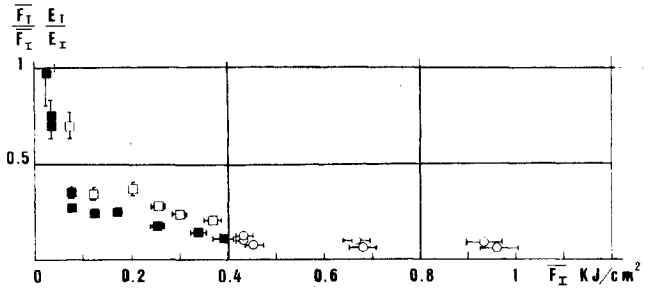


Fig. 4 Ratio of transmitted energy to incident energy as a function of incident fluence. Experimental conditions: $0<E_I<2$ kJ; ○ $f=13$ m, $S^*=0.24$ cm² and □ $f=62$ m, $S^*=2$ cm² at 10-11°C, 54-62% RH; ■ $f=62$ m, $S^*=2$ cm² at 8-9°C, 67-73% RH.

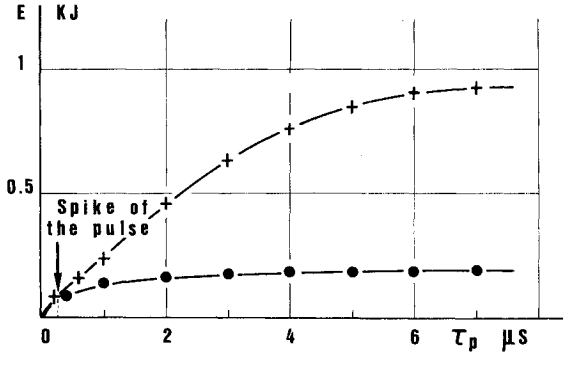


Fig. 5 Incident and transmitted laser energy as a fucntion of time. $E_I=920$ J and $\bar{F}_I=368$ J/cm² at 11°C and 54% RH; length of breakdown ≃6 m; + is incident energy, • transmitted energy.

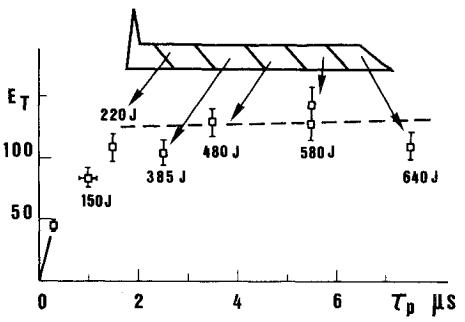


Fig. 6 Transmitted energy as a function of the laser pulse duration $\tau_p$. Experimental conditions: $f=62$ m, $f/D=103$, $S^*=2$ cm² at ≃10°C and 65% RH.

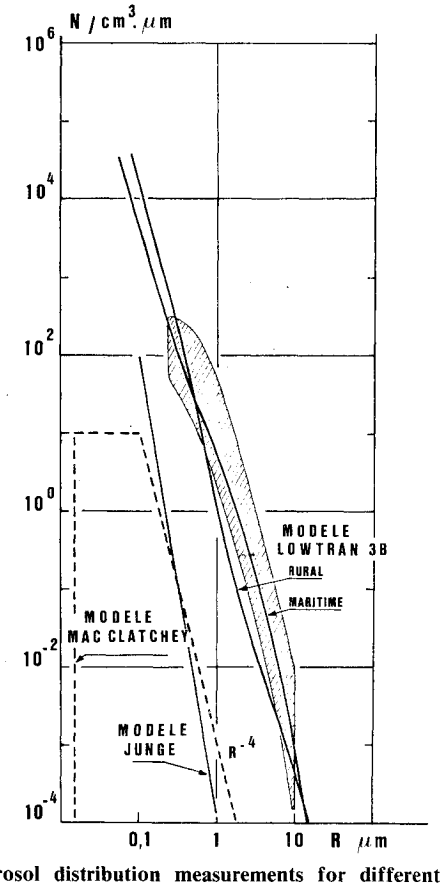


Fig. 7 Aerosol distribution measurements for different relative humidity and air temperature conditions: 15°C and 45% RH up to 4°C and 90% RH.

to the incident energy decreases when the incident fluence increases (for example, 25-30% for $\bar{F}_I=0.2$ kJ/cm² and 6% for $\bar{F}_I=1$ kJ/cm²).

**Temporal Effects**

For a given value of the fluence, it is possible to find the variations of the transmitted energy as a function of time (e.g., $E_I=920$ J, $\bar{F}_I=368$ J/cm²). See Fig. 5.

Note that the energy ($E_T=190$ J) is rapidly blocked due to the rapid development of the plasma. However, most of the transmitted energy comes from the spike (≃250 ns), $E_T=90$ J for $E_{I_{spike}}=110$ J). The laser energy transmitted through the plasma during the tail of the pulse is very weak ($E_T=10\%$ $E_I$).

To measure the transmitted energy as a function of the laser pulse duration, experiments have been carried out with different durations of the tail of the pulse (by varying the duration of the high-voltage discharge). In all the cases, the spike of the pulse is the same. The pulse duration range is 0.2-7.5 µs and the corresponding energy values range is 45-640 J ($\bar{F}_I=18$-256 J/cm²). We found that for $E_I>220$ J the transmitted energy does not increase. As an example, for $\tau_P=1.5$ µs ($E_I=220$ J), $E_T=109$ J and thus $E_T/E_I=49\%$; and for $\tau_P=7.5$ µs ($E_I=640$ J), $E_T=110$ J and $E_T/E_I=17\%$. These results are presented in Fig. 6. We can then determine the time of cutoff (≃1.5 µs) for a given set of conditions. After this cutoff time, the laser radiation is attenuated almost completely by the aerosol-induced plasma and the pulse duration must be limited to this time.

These experiments show that of the physical effects limiting the propagation of a high-fluence laser beam through the standard atmosphere, air breakdown is the most detrimental. With regard to the aerosol particles, the fundamental quantities required in the determination of the number of breakdowns and thus of the amount of energy absorption are

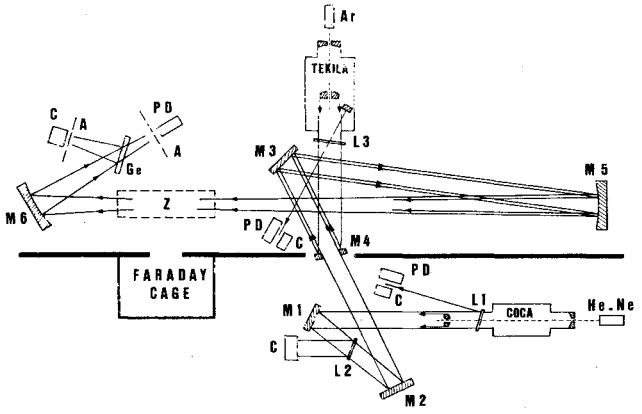


**Fig. 8 Experimental arrangement for double-pulse experiments. Key: A-attenuators; L1, L2, L3-NaCl windows; Ge-germanium beam splitter; PD-photon-drag detectors; C-calorimeters; Z-interaction zone; M1, M2, M3-plane mirrors; M4-annular plane mirror; M5, M6-concave spherical mirrors.**

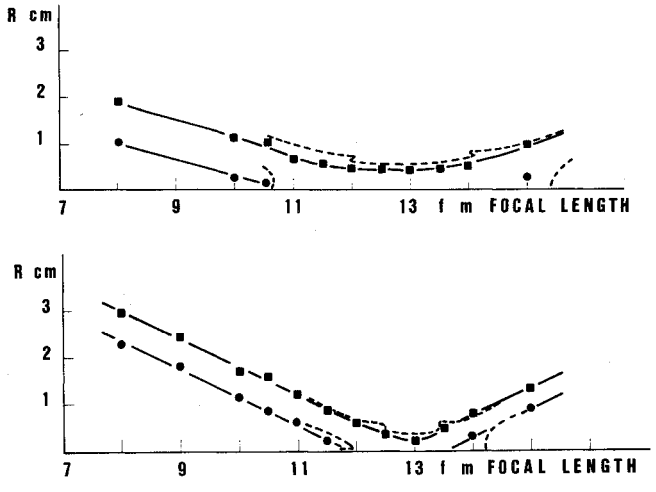


**Fig. 9 Isointensity contour in the focal region: a) the precursor pulse, $f/D = 130$; b) the second pulse, $f/D = 87$. ■ is external edge of the beam, • internal edge; the dotted line represents an isointensity contour (numerical result = 0.5% $I(o,F)$ where $I(o,F)$ = maximum intensity on the axis in the focal plane).**

the concentration and size distribution of the particles. These quantities have been measured using a particle counter, the "axially scattering spectrometer probe" (ASSP 100) that measures the 0.5-45 $\mu$m particle diameter in four ranges (0.5-7.5, 1-15, 2-30, and 3-45 $\mu$m), each being then equally divided into 15 linear size intervals. Size distribution measurements are quite difficult to perform because of the numerous interferring parameters: air temperature, relative humidity, barometric pressure, wind speed and direction, and the nature of the aerosol material (index of refraction), as well as the shape of the aerosols. Figure 7 shows the aerosol distribution measurements obtained for different relative humidity and air temperature conditions (hatched area). These measurements are compared to maritime and rural aerosol models (Lowtran 3B)[19] and to a $R^{-4}$ dependence model (MacClatchey, Junge). The number of particles per cm$^3/\mu$m is plotted in a log-log form as a function of the particle radius. The distribution function can be approximately represented by[10]

$$f(R) \simeq f_0 (R_1/R)^4 \text{ particles/cm}^3/\mu\text{m}$$

and

$$N_{\text{total}} = \int_{R_0}^{R_2} f(R)\,dR$$

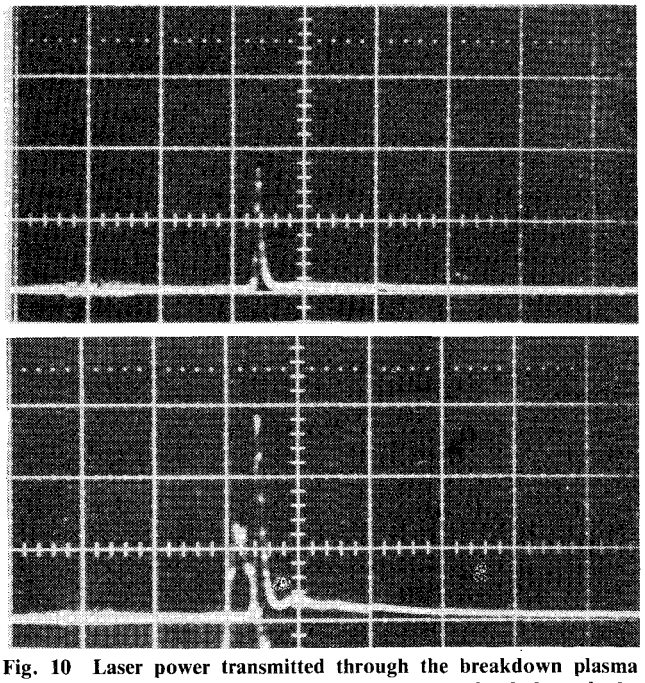

**Fig. 10 Laser power transmitted through the breakdown plasma without a precursor pulse: a) laser power transmitted through the cleaned zone; b) $\Delta t$ between the precursor and the second pulse = 100 $\mu$s; 1 $\mu$s/division. In this case, $\phi_T^+/\phi_T \simeq 1.6$ and $E_T^+/E_T \simeq 2.5$.**

where $R_0$ and $R_2$ are the small and large limits of the radius of the particles, respectively.

In order to estimate the number density above a critical radius (for determination of plasma breakdown number density), we have

$$N_{\text{critical}} = \int_{R_{\text{critical}}}^{R_2} f(R)\,dR$$

and

$$N_{\text{breakdown}} \leq N_{\text{critical}}$$

where $R_{\text{critical}}$ has been found[9] equal to 2 $\mu$m (any particles with a radius $>2$ $\mu$m can initiate the optical breakdown for intensities in the vicinity of $1\text{-}2\times10^8$ W/cm$^2$). The range of atmospheric conditions corresponding to our experiments (15°C, 45% RH to 4°C, 90% RH) is: $10^4$ $(10^{-1}/R)^4 \leq f(R) \leq 10^6$ $(10^{-1}/R)^4$, with $R$ in microns.

The upper edge of the hatched area of Fig. 7 corresponds to the higher humidity. Although the smaller particles ($R<5$ $\mu$m) are more numerous when the humidity is higher, for $R>5$ $\mu$m the error bars of the measurements of the number of particles are intermingling whatever the temperature and the humidity may be. Consequently, it is very difficult to interprete the number of breakdowns and, thus, the beam blockage as a function of the atmospheric conditions.

## Double-Pulse Experiments

Taking into account the high-energy absorption by the air plasma in the intensity ranges above $10^8$ W/cm$^2$ and fluence ranges above 5 J/cm$^2$, preliminary experiments have been performed inside the laboratory to study the possibility of increasing the transmitted energy by the application of a precursor pulse. Previously published studies have shown that the air breakdown threshold can be increased by the application of a precursor pulse of sufficient energy density.[20] In the case of a 50 $\mu$m diam carbon particle, the threshold breakdown has been increased by a factor of 19 (one-half of the clean air breakdown threshold). Consequently, the energy transmission will be better. The main mechanisms concerning this effect are the vaporization of the aqueous droplets[21-24] (important for small sizes) and the ejection out of the focal volume (important for large sizes). For instance, for large fog

droplets, front surface vaporization has been observed and partially varporized particles can be propelled with a maximum probability along a direction close to the initial direction of the laser beam.[25-27] The following experiments have been performed with the two previously described $CO_2$ lasers. These are individually controlled so that their initiation can be separated. The possibility of increasing the transmission of the incident energy has been studied as a function of the double-pulse separation time. This time is defined as that between the beginning of the two pulses (controllable from a few microseconds to 0.1 s). The experimental arrangement allows the coaxial propagation of the two laser beams. As Fig. 8 schematically shows, superposition of the two beams is obtained by use of the annular plane mirror $M_4$, and the two beams after are focused on the same focal volume by means of a single 13 m focal-length mirror ($f/D=130$, $S^*=0.53$ cm$^2$ for laser COCA; $f/D=87$, $S^*=0.24$ cm$^2$ for laser TEKILA). The experimental conditions are presented in Table 1.

In order to study the perfect superposition of the breakdown area, the cross-sectional intensity variations along the beam axis have been measured by burning (with nearly constant laser intensity) light-blackened photographic paper sheets. The envelope of the light rays of the second pulse is contained within that of the initial pulse over a distance of 2 m. This has been controlled by means of a video recordings and time-integrated photographs. Figure 9 shows the experimental determination of the isointensity contour in the focal region for the precursor pulse and the second pulse, respectively.

### Effect of Interpulse Time

These experiments determined the influence of the delay time $\Delta t$ between pulses on the transmission of the laser energy at the second pulse. $E_T^+$, the transmitted energy when there is a precursor pulse is compared with $E_T$, the transmitted energy without the precursor pulse. A similar comparison is made for the transmitted intensitites $\phi_T^+$ and $\phi_T$ (maximum intensity obtained at the top of the gain-switched spike of the pulse).

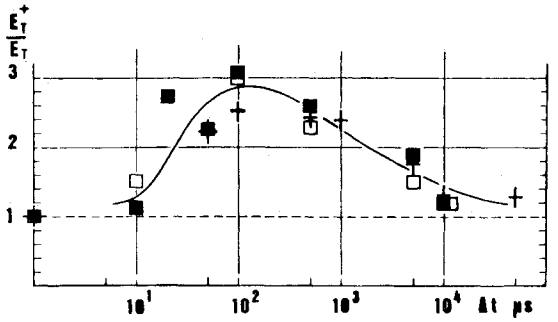


**Fig. 11 Separation time determination for which $E_T^+/E_T$ is maximum; $E_T^+$ = transmitted energy with precursor pulse; $E_T$ = transmitted energy without precursor pulse; +, □ are photon-drag measurements and ■ calorimeter measurements.**

**Table 1 Experimental conditions**

| Pulse, deg | $f$, m | $f/D$ | $S^*$, cm$^2$ | $\bar{\phi}_{peak}$, W/cm$^2$ | $\bar{\phi}_{tail}$, W/cm$^2$ | $\tau_{pulse}$, μs | $E_I$, J | $\bar{F}_I$, J/cm$^2$ |
|---|---|---|---|---|---|---|---|---|
| 1 | 13 | 130 | 0.53 | $4.5\times10^8$ | $1.0\times10^8$ | 2,5 | 100 | 150 |
| 2 | 13 | 87 | 0.24 | $8.0\times10^8$ | $1.5\times10^8$ | 5 | 130 | 430 |

Figure 10 contains oscillograms of laser pulses transmitted through the breakdown area when there is no precursor pulse and when a first pulse occurs 100 μs before the second pulse arises. Figures 11 and 12 show the beneficial effect of the precursor pulse. Results obtained from power (photon-drag detector) and energy (calorimeter) simultaneous measurements cover two series of experiments (+ designates series 1 and □ ■ series 2) performed under very similar atmospheric aerosol conditions. However, it has not been possible to measure the concentration of aerosols present in the breakdown zone (the conditions of air temperature and relative humidity were 20°C and 40%, respectively).

These experimental results show that the transmitted energy and the maximum transmitted intensity have been raised by a factor of 3 and 1.7, respectively, for a pulse separation time of 100-200 μs. With no prepulse the transmitted energy $E_T$ is approximately equal to 14 J ($\simeq 0.11\ E_I$). When the "cleaning" effect is maximum, the ratio $E_T^+/E_T$ is increased by up to 0.27-0.33 ($E_T^+ \simeq 40$ J).

### Long Interpulse Times

Generally, at $\Delta t$ ranges of 0-50 μs, the plasma initiated by the precursor pulse develops and absorbs the energy of the second pulse. When $\Delta t$ is larger than 5 ms, the effectiveness of the precursor pulse is less noticeable because of the return into the interaction zone of new aerosol particles that are capable of initiating breakdown again.

Thus, the transmitted energy $E_T^+$ and the transmitted intensity $\phi_T^+$ drop to their initial values. Actually, taking into account the zone cleaned up by the first pulse (diameter $\simeq 1$ cm), a transverse wind of 1 m/s can bring a particle back to the center of this zone within 5 ms. The influence of the diffusion and gravity is negligible because in 1 s a 1 μm particle diffuses a distance on the order of $4.10^{-4}$ cm, while it falls about $2.10^{-2}$ cm under the influence of gravity. A 10 μm particle has a falling speed of about 2 cm/s.

For a double-pulse separation time varying from 50 μs to 5 ms, the second pulse meets in the cleaned zone with a modified repartition and concentration of aerosols. A more thorough analysis will be performed to determine the importance of the various mechanisms interfering in this

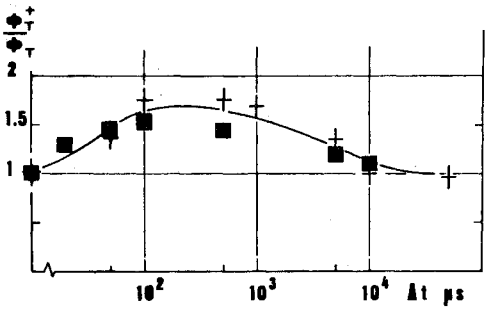


**Fig.12 Increase in the maximum transmitted intensity as a function of the double pulse separation time: + experiment 1; ■ experiments 2.**

**Table 2 Experimental conditions**

| $E_I$, J | $\bar{F}_I$, J/cm$^2$ | $\phi_T^+$, W/cm$^2$ | $\phi_T^+/\phi_T$ | $E_T^+$, J | $E_T^+/E_T$ | $E_T/E_I$, % | $E_T^+/E_I$ % | $\bar{F}_T^+$, J/cm$^2$ |
|---|---|---|---|---|---|---|---|---|
| 130 | 430 | $1.4\times10^8$ | 1.50 | 48 | 3 | 12.5 | 37 | 159 |
| 200 | 670 | $1.9\times10^8$ | 1.65 | 54 | 2.7 | 10 | 27 | 180 |
| 280 | 930 | $2.0\times10^8$ | 1.68 | 47.5 | 1.9 | 9 | 17 | 158 |

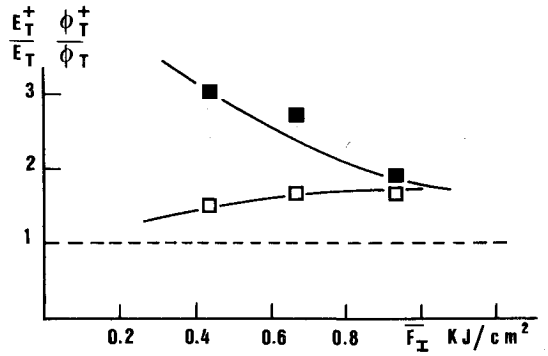


**Fig. 13 Cleaning effect as a function of the incident fluence of the second pulse: ■ $E_T^+/E_T$; □ $\phi_T^+/\phi_T$; double-pulse separation time $\Delta t = 100$ μs.**

cleaning effect (vaporization, ejection out of the focal volume, or fragmentation).

#### Effect of Second-Pulse Fluence

For a given value of the fluence of the precursor pulse (150 J/cm²) and for a given value of the separation time ($t = 100$ μs), the total energy transmitted through the cleaned zone as a function of the incident energy of the second pulse has been investigated. The experimental conditions are compiled in Table 2. These results are presented in Fig. 13.

We note a reduction of the "cleaning" effect when the incident fluence of the second pulse increases. Then, when the fluence increase, the length of the breakdown zone increases. Consequently, the focal volume of the second pulse cannot be completely contained in that of the precursor pulse (cleaned zone) and air breakdown can occur near the ends. This is an important limitation.

## Conclusion

When intensity and fluence levels are high enough to cause breakdown, an air plasma is created, leading to almost total laser energy absorption (transmission < 15% for $\bar{F}_I > 300$ J/cm²). Experiments presented in this paper have shown the possibility of increasing the transmission of the incident energy (by a factor of three) through the atmosphere by cleaning the path of the beam by means of a precursor pulse.

Experiments are now in progress in the laboratory to study the "cleaning" effect in a large focal volume over long distances and outside the laboratory with atmospheric aerosol concentration control.

## Acknowledgments

The authors would like to thank J-P. Fragassi for his assistance throughout the course of this work. This work is supported by the Direction des Recherches, Etudes et Techniques, under Contract 80-181.

## References

[1] Smith, D. C., "Gas Breakdown Dependence on Beam Size and Pulse Duration with 10.6 μm Wavelength Radiation," *Applied Physics Letters*, Vol. 19, Nov. 1971, pp. 405-408.

[2] Marquet, L. C., Hull, R. J., and Lencioni, D. E., "Studies of Breakdown in Air Induced by a Pulsed $CO_2$ Laser," *IEEE Journal of Quantum Electronics*, Vol. QE8, June 1972, p. 564.

[3] Lencioni, D. E., "The Effect of Dust on 10.6 μm Laser Induced Air Breakdown," *Applied Physics Letters*, Vol. 23, July 1973, pp. 12-14.

[4] Smith, D. C. and Brown, R. T., "Aerosol-Induced Air Breakdown with $CO_2$ Laser Radiation," *Journal of Applied Physics*, Vol. 46, March 1975, pp. 1146-1154.

[5] Lencioni, D. E., "The Limitations Imposed by Atmosphere Breakdown on the Propagation of High Power Laser Beam," *AGARD Conference Proceedings*, CP 183, Oct. 1975, pp. 32-1/32.12.

[6] Lencioni, D. E. and Pettingill, L. C., "The Dynamics of Air Breakdown Initiated by a Particle in a Laser Beam," *Journal of Applied Physics*, Vol. 48, May 1977, pp. 1848-1851.

[7] Smith, D. C., "Gas Breakdown Initiated by Laser Radiation Interaction with Aerosols and Solid Surfaces," *Journal of Applied Physics*, Vol. 48, June 1977, pp. 2217-2225.

[8] Reilly, J-P., Singh, P., and Weyl, G., "Multiple Pulse Laser Propagation through Atmosphere Dusts at 10.6 Microns," AIAA Paper presented at AIAA 10th Fluid and Plasma Dynamics Conference, Albuquerque, 1977.

[9] Autric, M., Caressa, J-P., Bournot, Ph., Dufresne, D., and M. Sarazin," Propagation of Pulsed Laser Energy Through the Atmosphere," *AIAA Journal*, Vol. 19, Nov. 1981, pp. 1415-1421.

[10] Reilly, J-P., Delichatsios, M., Glickler, S. L., Korff, D., Singh, P. I., and Weyl, G. M., "Multiple Pulse Propagation in Fog, Rain and Dust at 10.6 μm," Avco Everett Research Laboratories, Interim Rept. 173-76C 0059, July 1976.

[11] Greig, J. R., Pechacek, R. E., Fernsler, R. F., Vitkovitsky, I. M., Desilva, A. M., and Koopman, D. W., "A Preliminary Study of Aerosol Initiated $CO_2$ Laser Produced Air Sparks and Their Ability to Guide Electrical Discharge," NRL Memorandum Rept. 3647, Nov. 1977.

[12] Koopman, D., Greig, J., Pechacek, R., Ali, A., Vitkovitsky, I., and Fernsler, R., "$CO_2$-Laser Produced Channels for Guiding Long Spark in Air," *Journal de Physique*, Vol. 40, No. C7, July 1979, pp. C7-419-420.

[13] Singh, P. I., "Experiments on Aerosol Induced Breakdown by Pulsed Lasers," AIAA Paper 79-0249, Jan. 1979.

[14] Raizer, Yu. P., "Heating of a Gas by Powerful Light Pulse," *Soviet Physics-JETP*, Vol. 21, No. 5, Nov. 1965, pp. 1009-1017.

[15] Edwards, A. L. and Fleck, J. A. Jr., "Two-Dimensional Modeling of Aerosol-Induced Breakdown in Air," *Journal of Applied Physics*, Vol. 50, June 1979, pp. 4308-4313.

[16] Boni, A. A. and Su, F. Y., "An Analytical Technique for Laser-Driven Shock Waves," *Acta Astronautica*, Vol. 1, 1974, pp. 761-780.

[17] Vigliano, P., Autric, M., Caressa, J-P., Chhim, V., and Inglesakis, G., "Hydrodynamical Models of Aerosol-Induced Breakdown," *4th International Symposium on Gas Flow and Chemical Lasers*, Stresa, Italy, Sept. 1982, Paper 24.

[18] Autric, M., Caressa, J-P., Dufresne, D., and Bournot, Ph., "Etude Experimentale de La Propagation dans L'air d'une impulsion de haute energie émise par un Laser $CO_2$," *Comptes Rendus de l'Academie des Sciences, Paris*, Serie B, Vol. 288, April 1979, pp. 237-240.

[19] Shettle, E. P. and Fenn, R. W., "Models of the Atmospheric Aerosols and Their Optical Properties," *Optical Propagation in the Atmosphere*, AGARD CP-183, Oct. 1975, pp. 2.1-2.16.

[20] Lencioni, D. E. and Lowder, J. E., "Aerosol Clearing with a 10.6 μm Precursor Pulse," *IEEE Journal of Quantum Electronics*, Vol. QE10, Feb. 1974, pp. 235-238.

[21] Sutton, G. W., "Fog Dispersal by High-Power Lasers," *AIAA Journal*, Vol. 8, Oct. 1970, pp. 1907-1910.

[22] Glickler, S. L., "Propagation of a 10.6 μm Laser through a Cloud Including Droplet Varporization," *Applied Optics*, Vol. 10, March 1971, pp. 644-650.

[23] Lowder, J. E., Kleiman, H., and O'Neil, R. W., "High-Energy $CO_2$ Laser Pulse Transmission through Fog," *Journal of Applied Physics*, Vol. 45, Jan. 1974, pp. 221-223.

[24] Sutton, G. W., "Fog Hole Boring with Pulsed High-Energy Lasers: An Exact Solution Including Scattering and Absorption," *Applied Optics*, Vol. 17, No. 21, Nov. 1978, pp. 3424-3430.

[25] Pogodaev, V. A., Bukatyi, V. I., Khmelevtsov, S. S., and Chistyakova, L. K., "Dynamics of the Explosive Evaporation of Water Drops in the Field of Optical Radiation," *Soviet Journal of Quantum Electronics*, Vol. 1, No. 4, Jan.-Feb. 1972, pp. 422-424.

[26] Kafalas, P. and Ferdinand, A. P. Jr., "Fog Droplet Vaporization and Fragmentation by a 10.6 μm Laser Pulse," *Applied Optics*, Vol. 12, Jan. 1973, pp. 29-33.

[27] Kafalas, P. and Herrmann, J., "Dynamics and Energetics of the Explosive Vaporization of Fog Droplets by a 10.6 μm Laser Pulse," *Applied Optics*, Vol. 12, April 1973, pp. 772-775.